

PEDOT/Palladium composite material: synthesis, characterization and application to simultaneous determination of dopamine and uric acid

S. Harish · J. Mathiyarasu · K. L. N. Phani ·
V. Yegnaraman

Received: 17 December 2007 / Accepted: 16 May 2008 / Published online: 3 June 2008
© Springer Science+Business Media B.V. 2008

Abstract Palladium (Pd) incorporated poly (3,4-ethylenedioxythiophene) (PEDOT) films were synthesized through an electrochemical route and characterized using scanning electron microscopy (SEM) and atomic force microscopy (AFM). The electrochemical study showed catalytic oxidation of dopamine (DA) with optimum loading of Pd. DA and uric acid (UA) were detected using differential pulse voltammetry (DPV). In the presence of ascorbic acid (AA), DA-AA showed peak potential separation of 0.19 V while 0.32 V between UA-AA on Pd-incorporated PEDOT. These peak separations are large enough for sensing DA and UA in the presence of AA. DA and UA exhibited linear calibration plots and the minimum detection limits are 0.5 and 7 μM respectively. On Pd-PEDOT, the reversibility of DA oxidation was found to increase compared to bare glassy carbon electrode (GCE) and PEDOT modified GCE. Fouling effects were also found to be minimal making Pd-PEDOT composite suitable for electroanalysis.

Keywords Voltammetry · Dopamine · Uric acid · Palladium · PEDOT

1 Introduction

Conducting polymers are emerging as intelligent materials [1] and they are in the forefront of research in the synthetic chemistry of functionalized pi-conjugated systems. These

materials have a wide range of applications in the field of optical, electronic, electro-chromic devices, and sensors etc. Among the reported conducting polymer materials, poly (3,4-ethylenedioxythiophene) (PEDOT) is considered to be a promising candidate for its regioregular polymerization, low bandgap, stability and optical transparency [2–4]. The recent technological interests are in the synthesis of conducting polymers incorporated with metal nanoparticles for varied applications. Conducting polymers are widely employed as support materials for dispersing the metal particles and the resultant composite materials possess improved catalytic efficiency [5, 6]. The latter were widely used in the applications for oxidation of small organic molecules, dioxygen reduction etc [7–11].

Metal nanoparticle-incorporated PEDOT composite materials have been widely reported. Tsakova et al studied the crystallization of copper (Cu), Pd and bimetallic (Cu–Pd) in PEDOT matrix which was used for electroreduction of nitrate ions in neutral solutions [12–16]. Current-sensing atomic force microscopy showed that PEDOT with its sulfur atoms (having better aligned surface) form strong bonding with platinum (Pt), gold (Au) and silver (Ag) nanoparticles [17]. In lithium ion batteries, PEDOT incorporated with $\text{LiCoO}_2/\text{VS}_2$ composite material was used as a cathode material. These were reported to have good thermal and chemical stability, fast electrochemical switching and high electrical conductivity in the p-doped state [18, 19].

In our recent communications, we reported the utility of Au incorporated PEDOT in the sensing of DA and UA in the presence of excess AA [20–24] wherein PEDOT showed larger voltammetric peak separations. In continuation of this effort, we have attempted the synthesis of Pd incorporated PEDOT composite material for electroanalysis. Further, Pd nanoparticles are reported to be catalytic for several organic

S. Harish (✉) · J. Mathiyarasu · K. L. N. Phani ·
V. Yegnaraman
Electrodes and Electrocatalysis Division, Central
Electrochemical Research Institute, Karaikudi 630 006, India
e-mail: harish.srinivas@yahoo.com

reactions such as Heck, Suzuki, Kumuda etc., [25–27] and used as a material for detection of gaseous hydrogen [28], cholesterol [29], hydrazine [30] and dissolved oxygen [31].

The electrochemically synthesized Pd incorporated PEDOT matrix is characterized using surface analytical techniques. Besides, optimization of Pd loading into the polymeric films, their application to sensing of DA and UA in the presence of excess AA are demonstrated.

2 Experimental

2.1 Materials

3,4-Ethylenedioxythiophene (EDOT, Baytron M) was a gift sample provided by Bayer AG (Germany). PdCl₂ (E-Merck), Dopamine (Acros), Ascorbic acid (E-Merck), Uric acid (E-Merck), potassium dihydrogen phosphate (E-Merck), sodium hydroxide (E-Merck) were used as received.

The aqueous solutions were prepared using Milli-Q water (18.3 MΩ) (Millipore). A standard 3-electrode configuration consisting of GCE (ϕ 3 mm, BAS, Inc.) as working electrode and Pt foil as auxiliary electrode and Ag wire/Ag-AgCl reference electrodes were employed in electrochemical experiments.

2.2 Instrumentation

Electrochemical experiments were carried out using a potentiostat/galvanostat Autolab PGSTAT-30 (Eco-Chemie B.V., The Netherlands) at room temperature 25 ± 1 °C. To record the DPV, the following input parameters were used: scan rate: 0.012 mV s^{-1} , sample-width: 17 ms, pulse-amplitude: 25 mV, pulse-width (modulation time): 50 ms, pulse-period (interval): 500 ms and rest-time: 5 s. Peak currents were determined after subtraction of a manually added baseline. PEDOT/Pd-PEDOT films coated on Indium doped Tin Oxide (ITO) glass substrates (Donnelly Corp., USA) were characterized by AFM (Molecular Imaging, USA) using Au coated SiN₃ cantilevers (Force constant 3 N/W). SEM measurements were made using Hitachi Model S-3000H with 10 kV (acceleration voltage).

3 Results and discussions

3.1 Synthesis of PEDOT/Pd-PEDOT composites

Figure 1 shows the electrochemical synthesis of PEDOT from acetonitrile solution containing 0.01 M EDOT and 0.1 M tetrabutylammonium perchlorate (TBAPC) as supporting electrolyte. The potential window was -0.9 to

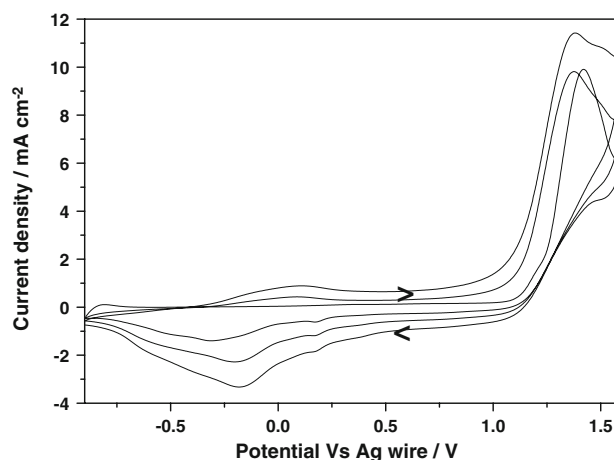


Fig. 1 Cyclic voltammogram showing the polymerization of 0.01 M EDOT in 0.1 M TBAPC on GCE from acetonitrile solution; Scan rate: 100 mV s^{-1}

1.6 V vs. Ag wire (reference electrode) and the scan rate used was 0.1 V s^{-1} . From the cyclic voltammogram, it was observed that EDOT oxidation starts at ~ 1.4 V and further cycling facilitates PEDOT film formation on the electrode surface. In order to obtain a thin film, PEDOT was allowed to grow on the GCE surface for three successive scans. This was seen from the increasing anodic and cathodic peak current densities at ~ 0.118 V and ~ -0.18 V during the forward and reverse scan, respectively.

Pd incorporated PEDOT composite films were synthesized as follows: PEDOT films initially synthesized from acetonitrile solution were kept at a potential of -0.1 V vs. MSE (Mercury/Mercurous sulfate electrode) for about 360 s in 0.5 M sulphuric acid containing palladium chloride. At this potential, the Pd²⁺ ions were reduced to Pd⁰ and incorporated into the polymer matrix. Figure 2 shows the redox

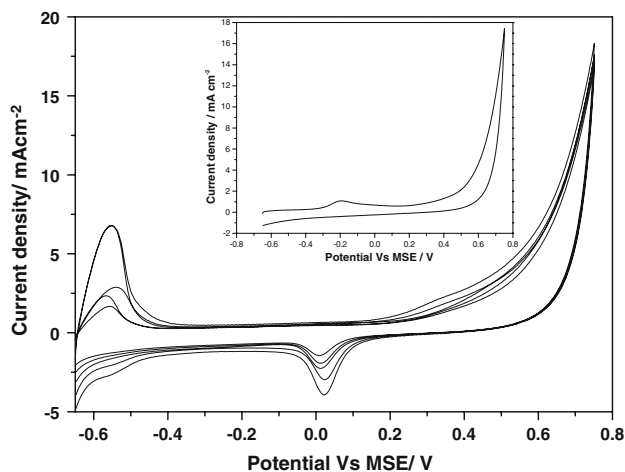


Fig. 2 Cyclic voltammogram showing the redox behaviour of Pd/PEDOT on GCE in 0.5 M H₂SO₄ solution; Scan rate: 100 mV s^{-1} (inset: Cyclic voltammogram shows the redox behaviour of PEDOT on GCE in 0.5 M H₂SO₄ solution)

behaviour of Pd incorporated PEDOT composite film in 0.5 M sulphuric acid and the inset shows the redox behaviour of PEDOT alone. The voltammetric features clearly show the redox characteristic of Pd that confirms its incorporation in the polymer matrix whereas it is absent in PEDOT alone. The hydrogen adsorption–desorption regions were also observed in this potential region. Further, the increase in Pd content in the polymer film is reflected by an increase in the reduction current as shown in the voltammograms.

3.2 Scanning electron microscopy

Figure 3 shows the SEM images of PEDOT and Pd-PEDOT composite films electrodeposited on an ITO glass substrate. PEDOT (Fig. 3a) deposited from the non-aqueous medium showed a uniform by sized fibrillar network structure with a fiber dimension of ~ 20 nm. These structures were not obtained when synthesized from a microemulsion or aqueous medium [14–16, 33]. The

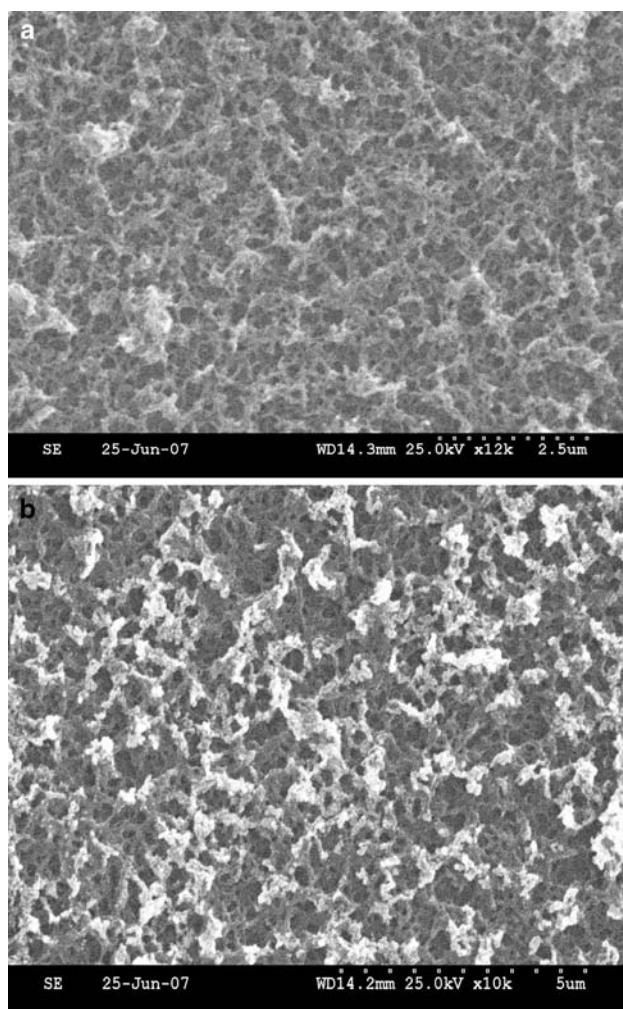


Fig. 3 SEM images of (a) PEDOT & (b) Pd/PEDOT coated on ITO glass substrate

polymer network has a highly porous structure that can easily entrap the foreign material yielding a composite. The image of PEDOT after Pd incorporation showed that the structure and morphology of the polymer film changed significantly. The regions where Pd is deposited clearly showed discrete areas of high contrast, suggesting the presence of Pd due to its conductivity difference. As can be seen from Fig. 3b, the fibrils containing Pd deposit retain a high porosity fibrillar network structure.

3.3 Atomic force microscopy

Figure 4 shows AFM images of PEDOT and Pd-PEDOT films electrochemically deposited on an ITO glass. Since the SEM figures do not show high contrast images, AFM analysis of the composite material was undertaken in this study. The corresponding 3D analyses of the films are also shown in Fig. 4. The PEDOT image (Fig. 4a) of $2 \times 2 \mu\text{m}$ shows a fibrillar network as seen in the SEM images. The PEDOT polymer is arranged in an array type structure and resulting in a network fibrillar structure. From the 3D analysis, it can be observed that the porous structure of the polymer film and the polymer fibril sizes are uniform for the area analyzed. Estimation of surface roughness of the polymer film was carried out and the mean value of roughness (R_a) was calculated as the deviations in height from the profile mean value

$$R_a = 1/N \sum_{i=1}^N |Z_i - Z| \quad (1)$$

where Z , is the sum of all height values divided by the number of data points (N) in the profile. The mean roughness value, estimated from these images using Eq. 1 is 4.6 nm.

Pd-incorporated composite polymer film (Fig. 4b) clearly shows morphological feature different from that of the polymer film alone. Pd incorporation results in the formation of a composite as is evidenced by the 3D image. Further, it is interesting to note that the mean surface roughness calculated for the composite film shows a value of 4.9 nm. This indicates that the surface porosity of the film does not change much upon incorporation of Pd.

3.4 Electrocatalytic oxidation of composite film

Figure 5 shows the cyclic voltammograms of 0.5 mM DA oxidation in a phosphate buffer solution (PBS 7.4) on bare GCE, GCE | PEDOT and GCE | Pd-PEDOT electrodes. On bare GCE, DA was oxidized at around 0.205 V yielding a peak current of $16 \pm 2 \mu\text{A}$, while a reduction peak at around 0.112 V was observed on the reverse scan. The peak separation ($E_{\text{aDA}} - E_{\text{cDA}}$, $\Delta E_p = 0.093 \pm 0.002$ V) suggests quasi-reversible nature of the oxidation process. On GCE | PEDOT, DA undergoes oxidation at around

Fig. 4 AFM images of (a) PEDOT & (b) Pd/PEDOT coated on ITO glass substrate

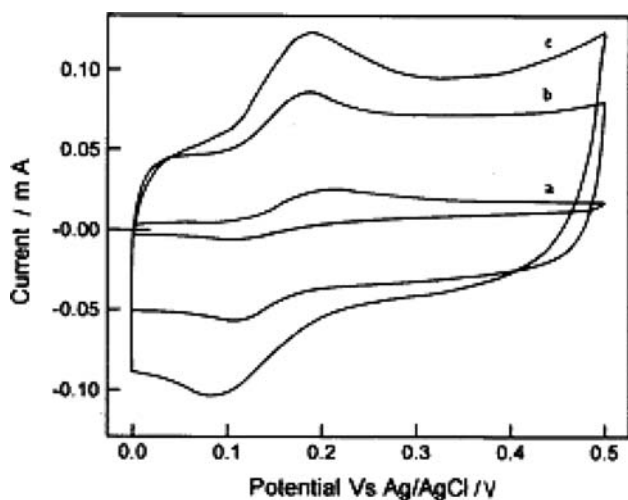
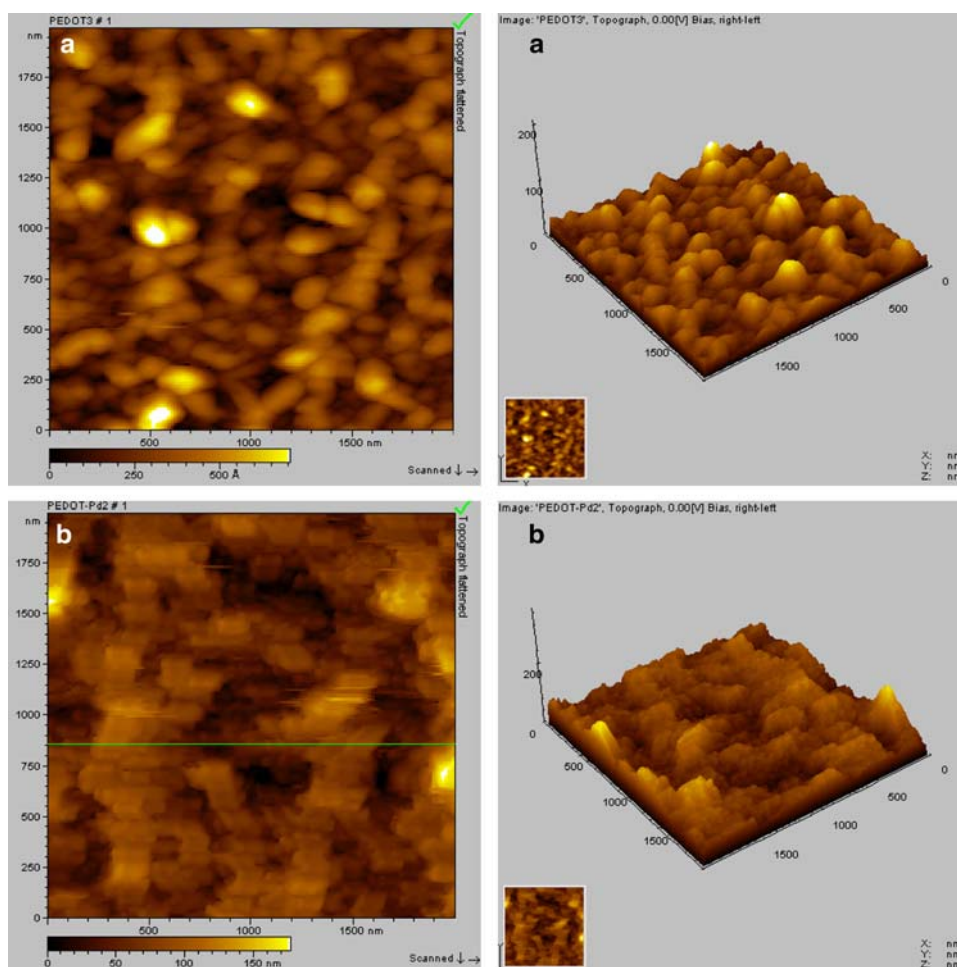


Fig. 5 Cyclic voltammogram of DA oxidation on (a) bare GCE (b) PEDOT/GCE (c) Pd/PEDOT/ GCE in neutral PBS 7.4

0.180 V, yielding a peak current of $29 \pm 2 \mu\text{A}$. When compared to bare GCE, appreciable potential shift for the DA oxidation on GCE | PEDOT was observed. The oxidation current increased by 1.8 times, indicating

catalytic oxidation of DA on the modified electrode. During the reverse scan, a cathodic peak and ΔE_p of 0.112 V and 0.068 ± 0.002 V, respectively, were observed which corresponds to a near-reversible process. Upon Pd incorporation within the polymer matrix, the DA oxidation occurs at 0.174 V with an oxidation current of $51 \pm 2 \mu\text{A}$ showing the improved catalytic behaviour of the composite film compared to PEDOT modified and bare GCE. During the reverse scan it also showed a peak at 0.1 V and the ΔE_p was found to be 0.074 V indicating the reversibility of the DA oxidation process. The reversible process indicates that DA oxidation on the composite electrodes does not cause electrode fouling. This is a serious problem faced in the analytical determination which in turn affects the precision.

3.5 Effect of Pd loading

To find the optimum loading of Pd in PEDOT that exhibits higher catalytic activity, polymer films containing various loadings of Pd were synthesized. In order to vary the Pd loading in the polymer film, the precursor i.e., palladium chloride concentration in the deposition solution was

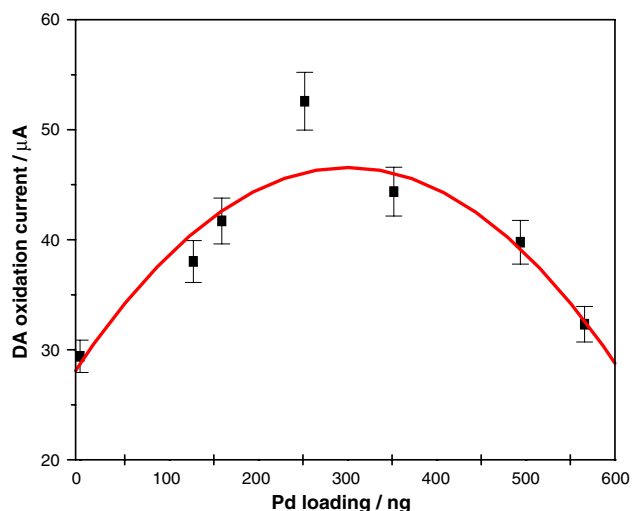


Fig. 6 Effect of palladium loading on PEDOT and its catalytic activity

varied. The amount of Pd in the film was calculated based on the integration of the hydrogen adsorption region. Figure 6 shows the DA oxidation current against amount of Pd loading in the film. The DA oxidation current increases with Pd loading up to ~ 250 ng and decreases after the critical loading. Pd loading corresponding to higher catalytic oxidation of DA was taken as the *threshold Pd loading* and used for DPV analysis.

3.6 Simultaneous determination of DA and UA

Detection of DA and UA concentration in biological samples in the presence of other constituents is an important task in clinical research [33–36]. DA and UA co-exist in biological samples along with other constituents in which AA is the excess amount compared to other molecules. Therefore, the detection of DA and UA in the presence of excess AA is of great importance.

Cyclic voltammetric studies of DA and UA oxidation on bare GCE in the presence of excess AA showed a broad and overlapping anodic peak (Figures not included). In contrast, PEDOT-GCE showed well-defined voltammetric peaks for each analyte. In order to improve the catalytic function, metal was entrapped into the polymer matrix and for this reason Pd was incorporated into the PEDOT film. The separation among the peaks was quite large which paved the way for simultaneous/selective determination of these biologically important molecules.

The electrooxidation of DA and UA in the presence of excess AA was investigated simultaneously by varying the concentration of the individual analyte species. The DPV technique was adopted because it has a much higher current sensitivity and better resolution than cyclic voltammetry. Moreover, the charging current contribution to the background current is the limiting factor in analytical

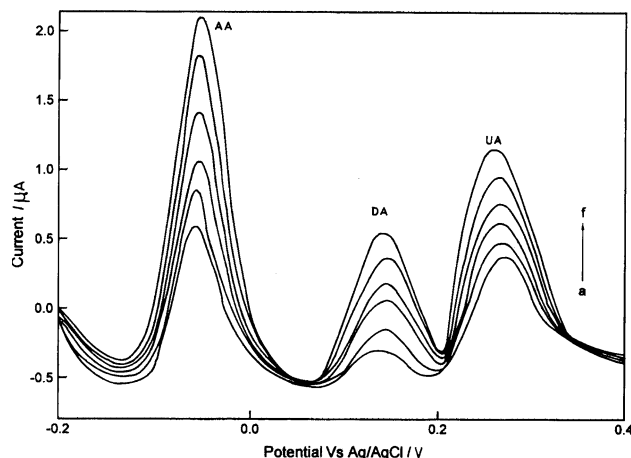


Fig. 7 Differential pulse Voltammogram of DA and UA oxidation in neutral PBS 7.4

determination whereas it was negligible in DPV mode [37]. Figure 7 shows the DPV of DA and UA in the presence of excess AA in PBS 7.4 on Pd-PEDOT modified GCE. The peak potential separations observed between DA-AA and UA-AA were 0.19 V and 0.32 V, respectively. This separation was well suited for DA and UA sensing in the presence of excess AA. Peak current was found to increase with concentration of the individual analyte molecule. Figure 8 shows calibration curves obtained using DPV. These exhibit a linear relationship between catalytic peak current and analyte concentration over a range of 0.5–1.0 and 7–11 μM for DA and UA, respectively. The calibration plots were found to be linear. For DA, the correlation coefficient (R^2) was 0.99 with 0.0019 $\mu\text{A}/\text{nM}$ slope while for UA, R^2 was 0.99 with 0.1979 $\mu\text{A}/\mu\text{M}$ slope. Thus, the polymer film showed improved properties for sensing applications in terms of selectivity and sensitivity compared to the individual materials respectively.

4 Conclusions

Pd-PEDOT films were prepared electrochemically and characterized using SEM and AFM techniques. PEDOT alone has a fibrillar network structure and Pd was incorporated within the porous polymer network structure. Pd-PEDOT composite material was used for sensing DA and UA in the presence of excess AA. Compared to bare GCE and PEDOT alone, Pd incorporated PEDOT showed excellent catalytic activity towards DA oxidation. The reversibility of DA oxidation on Pd-PEDOT film was considerably improved and hence the composite-modified electrode does not suffer from fouling due to the products of DA oxidation. Pd-PEDOT composite film enables detection up to 0.5 μM of DA and 7.0 μM of UA. Good linear correlations between oxidation current and DA and

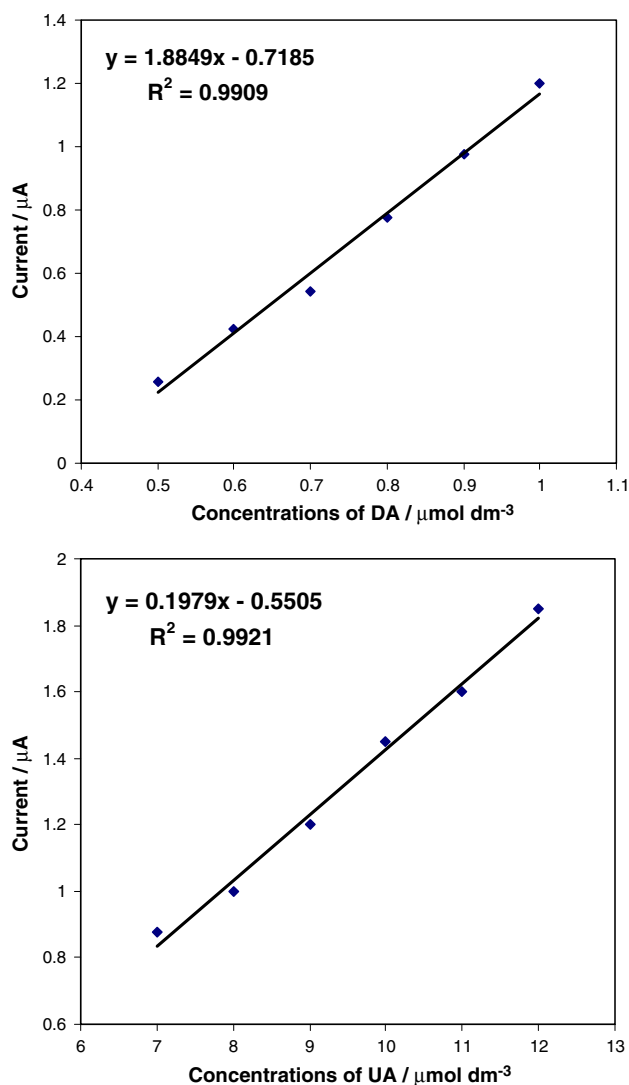


Fig. 8 Calibration curves of DA and UA

UA concentrations were obtained. As a result Pd-PEDOT shows more sensitivity and selectivity towards DA and UA in the presence of excess AA when compared to PEDOT.

Acknowledgments S. Harish thanks C.S.I.R., New Delhi for the award of Research Internship.

References

1. Lyons MEG (1994) In: Lyons MEG (ed) *Electroactive polymer electrochemistry, Part I*. Plenum Press, New York

2. Gronendaal LB, Jonas F, Freitag D, Pielartzik H, Reynolds JR (2000) *Adv Mater* 12:481
3. Roncali J, Blanchard P, Frère P (2005) *J Mater Chem* 15:1589
4. Kumar A, Buyukmumcu Z, Sotzing GA (2006) *Macromolecules* 39:2723
5. Biallozor S, Kupnieszka A, Jasulajtene V (2004) *B Electrochem* 20:231
6. Niu L, Li Q, Wei F, Chen X, Wang H (2003) *Synth Met* 139:271
7. LakshmiKantam M, Roy M, Roy S, Sreedhar B, Madhavendra SS, Choudary BM, De RL (2007) *Tetrahedron* 63:8002
8. Dodouche I, Epron F (2007) *Appl Catal B: Environ* 76:291
9. Serov AA, Cho SY, Han S, Min M, Chai G, Nam KH, Kwak C (2007) *Electrochem Commun* 9:2041
10. Tarasevich MR, Zhutaeva GV, Bogdanovskaya VA, Radina MV, Ehrenburg MR, Chalykh AE (2007) *Electrochim Acta* 52:5108
11. Bashyam R, Zelenay P (2006) *Nature* 443:6
12. Tsakova V, Winkels S, Schultze JW (2001) *J Electroanal Chem* 500:574
13. Ilieva M, Tsakova V (2004) *Synth Met* 141:287
14. Ilieva M, Tsakova V (2004) *Synth Met* 141:281
15. Ilieva M, Tsakova V (2005) *Electrochim Acta* 50:1669
16. Ilieva M, Tsakova V, Erfurth W (2006) *Electrochim Acta* 52:816
17. Cho SH, Park SM (2006) *J Phys Chem B* 110:25656
18. Murugan AV, Gopinath CS, Vijayamohan K (2005) *Electrochem Commun* 7:213
19. Her LJ, Hong JL, Chang CC (2006) *J Power Sources* 157:457
20. Mathiyarasu J, Kumar SS, Phani KLN, Yegnaraman V (2007) *J Nanosci Nanotechnol* 7:2206
21. Kumar SS, Mathiyarasu J, Phani KLN, Jain YK, Yegnaraman V (2005) *Electroanalysis* 17:2281
22. Radhajeyalakshmi S, Kumar SS, Mathiyarasu J, Phani KLN, Yegnaraman V (2007) *Ind J Chem* 46:957
23. Kumar SS, Mathiyarasu J, Phani KLN (2005) *J Electroanal Chem* 578:95
24. Kumar SS, Mathiyarasu J, Phani KLN, Yegnaraman V (2006) *J Solid State Electrochem* 10:905
25. Liu WJ, Xie YX, Liang Y, Li JH (2006) *Synthesis* 8:860
26. Karimi B, Enders D (2006) *Org Lett* 8:1237
27. Ackermann L, Althammer A (2006) *Org Lett* 8:3457
28. Yu S, Welp U, Hua LZ, Rydh A, Kwok WK, Wang HH (2007) *Chem Mater* 17:3445
29. Dong S, Deng Q, Cheng G (1993) *Anal Chim Acta* 279:235
30. Yang C, Senthil Kumar A, Kuo M, Chien S, Zen J (2005) *Anal Chim Acta* 554:66
31. Yang C, Senthil Kumar A, Zen J (2006) *Electroanalysis* 18:64
32. Han D, Yang G, Song J, Niu L, Ivaska A (2007) *J Electroanal Chem* 602:24
33. Li Y, Lin X (2006) *Sensor Actuat B-Chem* 115:134
34. Aguilar R, Dávila MM, Elizalde MP, Mattusch J, Wennrich R (2004) *Electrochim Acta* 49:851
35. Zen JM, Hsu CT, Hsu YL, Sue JW, Conte ED (2004) *Anal Chem* 76:4251
36. Zare HR, Rajabzadeh N, Nasirizadeh N, Ardakani MM (2006) *J Electroanal Chem* 589:60
37. Wang J (2000) *Analytical electrochemistry*. (Second Ed.), Wiley-VCH, New York